EJN European Journal of Neuroscience

FENS Federation of European Neuroscience Societies

European Journal of Neuroscience, Vol. 41, pp. 856–865, 2015 doi:10.1111/ejn.12842

COGNITIVE NEUROSCIENCE

Spatio-temporal response properties of local field potentials in the primate superior colliculus

Takuro Ikeda, Susan E. Boehnke, Robert A. Marino, Brian J. White, Chin-An Wang, Ron Levy and Douglas P. Munoz

Centre for Neuroscience Studies, Botterell Hall, Queen's University, 18 Stuart Street, Kingston, K7L 3N6, ON, Canada

Keywords: eye movements, rhesus monkey (*Macaca mulatta*), saccade, single unit activity, vision

Abstract

Local field potentials (LFPs) are becoming increasingly popular in neurophysiological studies. However, to date, most of the knowledge about LFPs has been obtained from cortical recordings. Here, we recorded single unit activity (SUA) and LFPs simultaneously from the superior colliculus (SC) of behaving rhesus monkeys. The SC is a midbrain structure that plays a central role in the visual orienting response. Previous studies have characterised the visual and visuomotor response properties of SUA in the superficial layers of the SC and the intermediate layers of the SC, respectively. We found that the signal properties of SUA were well preserved in the LFPs recorded from the SC. The SUA and LFPs had similar spatial and temporal properties, and the response properties of LFPs differed across layers, i.e. purely visual in the superficial layers of the SC but showing significant motor responses in the intermediate layers of the SC. There were also differences between SUA and LFPs. LFPs showed a significant reversal of activity following the phasic visual response, suggesting that the neighboring neurons were suppressed. The results indicate that the LFP can be used as a reliable measure of the SC activity in lieu of SUA, and open up a new way to assess sensorimotor processing within the SC.

Introduction

The superior colliculus (SC) coordinates the visual orienting response, which converts sensory information into motor commands for orienting the visual axis (Boehnke & Munoz, 2008; Gandhi & Katnani, 2011; Knudsen, 2011; Corneil & Munoz, 2014). Extensive research over the past few decades has revealed the detailed discharge characteristics of the neurons in the SC. The dorsal superficial layers of the SC (SCs) contain neurons that receive visual inputs from the retina (Wässle & Illing, 1980; Perry & Cowey, 1984) and visual cortices (Fries, 1984; Lui *et al.*, 1995). These SCs neurons are organised into a retinotopically coded map of the contralateral visual field (Cynader & Berman, 1972). However, the intermediate layers of the SC (SCi) receive converging sensory and cognitive information from various regions, such as the SCs (Moschovakis *et al.*, 1988; Behan & Appell, 1992; Lee *et al.*, 1997), basal ganglia (Graybiel, 1978; Hikosaka & Wurtz, 1983a), and the prefrontal, parietal and temporal cortices (Kuypers & Lawrence, 1967; Fries, 1984; Selemon & Goldman-Rakic, 1988), and integrate those input signals to produce motor commands to control eye movements and orienting (Gandhi & Katnani, 2011; Corneil & Munoz, 2014). However, little is known about how the SC neurons interact with each other to integrate sensory and cognitive information. Recording the local field potential (LFP) provides a strategy to address this question.

Correspondence: Douglas P. Munoz, as above.
E-mail: doug.munoz@queensu.ca

Received 17 December 2014, accepted 23 December 2014

The LFP represents the extracellular potential, which consists mainly of the sum of the post-synaptic potentials of neighboring neurons (Mitzdorf, 1985; Buzsáki, 2004; Logothetis & Wandell, 2004; Buzsáki *et al.*, 2012). LFPs are becoming popular targets of neurophysiological recordings in the cerebral cortex, because LFPs are suitable for simultaneous recordings from various areas and laminae, which enables the study of neural interactions (Buzsáki, 2004; Einevoll *et al.*, 2013); and the LFPs can capture synaptic processes that cannot be measured by conventional single unit activity (SUA) recordings (Bullock, 1997; Buzsáki, 2004; Logothetis & Wandell, 2004; Buzsáki *et al.*, 2012; Haider *et al.*, 2013). However, the nature of LFP signals in subcortical areas in primates remains largely unexplored. Here, we compared simultaneously recorded SUA and LFPs to identify similarities and differences between the two types of signal. We first examined the spatio-temporal properties of LFPs to test whether LFPs can be used as a reliable measure of sensorimotor processes in the SC. We then describe and interpret differences between SUA and LFPs. This is the first study analysing LFPs in the SC of behaving non-human primates and will provide a foundation for future research.

Materials and methods

All procedures were approved by the Queen's University Animal Care Committee and were in full compliance with the Canadian Council on Animal Care guidelines on the care and use of laboratory animals. Experiments were performed with three male rhesus monkeys (*Macaca mulatta*). Surgical procedures were described

previously (Marino *et al.*, 2008). Briefly, monkeys were implanted with a head post and a recording chamber over the SC, and eye coils were surgically implanted to measure eye position using the scleral search coil technique (Robinson, 1963). Surgery was performed under isoflurane anesthesia (2–2.5%) and the heart rate, pulse, pulse oximetry saturation, respiration rate, fluid levels, circulation and temperature were monitored throughout the surgical procedure. Monkeys were given 4 or more weeks to recover prior to behavioral training.

Behavioral paradigms

The behavioral paradigms and visual displays were controlled by REX version 6.1 (National Eye Institute, NIH, Bethesda, MD, USA). Monkeys were seated in a primate chair in front of a cathode ray tube monitor (75 Hz refresh rate, 71.5 × 53.5 cm; visual area 54 × 44°). The visual stimuli were presented in a dark environment. To prevent dark adaptation, the monitor was dimly illuminated (approximately 2 cd/m^2) during the intertrial interval (800–1500 ms). The monkeys were trained to perform four types of conventional saccade tasks: step, gap, visual delay and memory delay. All tasks required the monkeys to make a saccadic eye movement to the location of a visual stimulus (0.5° diameter spot, 42.5 cd/m^2) presented in one of two possible locations against a black background (approximately 0.0001 cd/m^2) either immediately (step and gap) or after a delay (visual delay and memory delay). One of the two possible target locations was set in the optimal location in the response field (RF) of the recorded neuron (Marino *et al.*, 2012) and the other was set at the horizontally and vertically opposite position (anti-RF location). These four tasks were randomly interleaved in a block of trials, with the two possible target locations kept constant during the block (50–120 trials in a block in most of the cases, more than 400 in some blocks). In some recording sessions, we only used visual delay and memory delay tasks.

To dissociate visual and motor activity, we analysed signals recorded in the visual delay and memory delay tasks (Fig. 1A and B). In these tasks, monkeys were required to fixate on the central fixation point for a variable period (500–800 ms) before the visual stimulus was presented. In the visual delay task, the stimulus remained on the screen and monkeys were required to keep central fixation for an additional 500–800 ms until the fixation point disappeared. Once the fixation point disappeared, the monkeys were required to make a saccade to the stimulus location to obtain a liquid reward. In the memory delay task, the visual stimulus was presented only briefly (93 ms) and monkeys were required to remember the location of the stimulus for 500–800 ms while maintaining central fixation. After the disappearance of the fixation point, monkeys were required to make a saccade to the remembered location to obtain a liquid reward. We used longer delay periods (1000–1300 ms) in several blocks, but a longer delay did not affect the neural response to the visual stimulus.

We used a visual mapping task to test the spatial properties of SUA and LFPs (Marino *et al.*, 2012). In this task, monkeys were required to maintain steady fixation on the central fixation point for approximately 4 s. During this fixation, brief flashes of white light (0.5° diameter spot, 42.5 cd/m^2, duration 93 ms) were presented sequentially in a pseudorandom order at one of 182 locations covering the entire visual field (horizontal 60°; vertical 50°) with an interstimulus interval of 147 ms. To avoid stimulating the same neuronal population repetitively, no two subsequent flashes within 10° eccentricity were presented within 10° of each other, and no two subsequent flashes beyond 10° eccentricity were presented within 20° of each other.

Data collection

Extracellular recording was performed with tungsten microelectrodes (0.5–2 MΩ impedance, Frederick Haer) inserted through guide tubes. Electrodes were advanced to the SC using a microdrive (Narishige, Tokyo, Japan). The dorsal surface of the SC was distinguished by large increases in multiunit activity following the presentation of visual stimuli. The depth of the recording site was defined as a depth relative to this surface point. We used this depth measurement as a rough estimate of the layer structure in the SC, as the measurement was not very accurate due to the variability in the recording conditions and isolation of neurons. Electrophysiological signals were recorded with a data acquisition system (Plexon Inc., Dallas, TX, USA). SUA signals were recorded at 40 kHz and amplified and filtered between 150 Hz and 8 kHz. SUA was isolated online using a window discriminator and confirmed offline using the Offline Sorter (Plexon Inc.). LFP signals were digitised at 1 kHz after filtering (0.7 Hz–8 kHz). The horizontal and vertical eye position was recorded using the magnetic search coil technique and sampled at 1 kHz (Robinson, 1963).

Data analysis

All analyses were performed offline with custom software written in MATLAB (Mathworks, Natick, MA, USA) using the Fieldtrip open source MATLAB toolbox (Oostenveld *et al.*, 2011). The eye velocity was calculated offline by the two-point central difference algorithm (Bahill *et al.*, 1982) and saccades were detected when the eye velocity of the polar component exceeded 80°/s after fixation point disappearance. The onset time of a saccade was then defined as the time point at which the velocity exceeded 35°/s, before reaching 80°/s.

As the SUA is a discrete representation of the timing of an action potential, it is difficult to compare SUA directly with the simultaneously recorded LFP, which is a continuous measure of activity. Therefore, we constructed spike density functions by convolving individual spikes with an excitatory post-synaptic potential-like function (Thompson *et al.*, 1996) (growth phase time constant, 1 ms; decay phase time constant, 20 ms). The excitatory post-synaptic potential-like kernel is better in temporal resolution compared with the Gaussian kernel, which usually brings the onset of the response a few milliseconds earlier. The resulting spike density function is a continuous signal that represents the onset of spiking activity at a resolution of 1 ms and was used to represent SUA. LFPs were aligned to stimulus appearance or saccade onset for each trial and those event-related LFPs were filtered using a low-pass filter (fourth-order Butterworth filter, bidirectional, cut-off, 50 Hz) to remove the potential influence of spiking activity (Zanos *et al.*, 2011), which also removed line noise at 60 Hz from power. The trials in which the LFP showed significant noise (typically > 5 SD $\pm$ mean) were excluded by visual inspection for all subsequent analyses. For population analysis, both SUA and LFPs were normalised so that the average baseline activity ($\pm$25 ms around stimulus appearance) was set to 0 and the peak activity of the phasic visual response (50–150 ms after stimulus appearance) was set to 1 in the visual delay task. Note that, because the LFPs had peak responses with negative values, the normalised LFPs were in the opposite direction to the raw LFP signals.

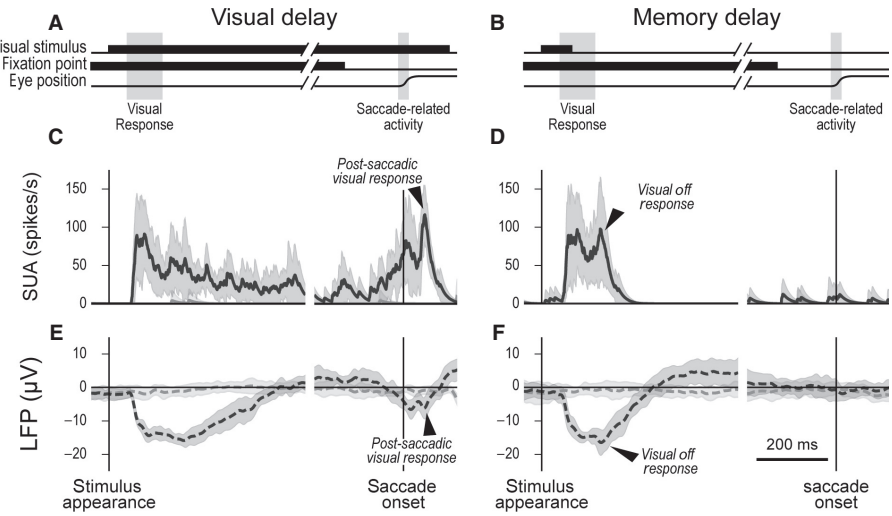

FIG. 1. (A and B) Schematic representation of visual delay and memory delay tasks, respectively. Shaded areas indicate the time windows used to analyse the visual response (50–150 ms after stimulus appearance) and saccade-related activity (±15 ms around saccade onset) to classify neurons. (C–F) An example of simultaneous recording of SUA and LFP. Signals were aligned to the stimulus appearance (left side) and saccade onset (right side). Black lines indicate the activity when the stimulus was presented in the RF in the contralateral visual field and gray lines indicate the activity when the stimulus was presented in the anti-RF in the ipsilateral visual field. Shaded area represents the SD. SUA (solid lines) in the visual delay (C) and memory delay (D) task; LFP (dashed lines) in the visual delay (E) and memory delay (F) task.

Cell classification

We classified neurons based upon their visual responses and saccade-related activity in the visual delay task (Fig. 1A). The visual response was defined as significantly higher SUA during the epoch 50–150 ms after visual stimulus appearance in the RF, compared with when the stimulus was presented in the anti-RF ($P < 0.05$, Mann–Whitney *U*-test). Saccade-related activity was defined as significantly higher SUA around saccade onset (±15 ms, baseline corrected with average pre-saccadic activity during 100–50 ms before saccade onset for each trial) when the monkeys made saccades to the RF, compared with when the monkeys made saccades to the anti-RF ($P < 0.05$, Mann–Whitney *U*-test). All of the neurons recorded had a visual response in both the visual and memory delay tasks. The neurons were classified into two types by their saccade-related activity in the visual delay task, i.e. visual (VIS) neurons with no significant saccade-related activity and visuomotor (VM) neurons with saccade-related activity. To compare the visuomotor properties of signals, we calculated the visuomotor index for SUA and LFP in each session. The visuomotor index was defined by the following formula

$$\text{Visuomotor Index} = \frac{V - M}{V + M}$$

where V is the average activity during the 50–150 ms epoch after visual stimulus appearance in the RF, and M is the average activity around saccade onset toward the RF (±15 ms). This index ranges from −1 (pure movement neuron) to +1 (pure visual neuron) for SUA; however, the index can be >1 or <−1 for LFP, as LFP can be both positive and negative.

Visual response onset latency

The onset of the visual response was determined as the time when the neural activity (SUA and LFPs) first became significantly different ($P < 0.01$, one-tailed paired *t*-test) from the baseline activity (average activity during −50 to 0 ms relative to the stimulus appearance) and remained so for ≥ 10 ms, following the stimulus appearance.

Visual response field

To study the spatial properties of SUA and LFP, we constructed a spatial response map from the data recorded in the visual mapping task. SUA and LFP were aligned to each stimulus appearance and the activity level was calculated for each location across the visual field according to the gaze-centered stimulus location, corrected for the average baseline activity ±25 ms around stimulus appearance. The response map was then smoothed by natural neighbor interpolation to construct a visual response map (0.5° grid) for each millisecond. The center of the visual RF was determined by the peak response point on the grid (average response during 50–150 ms after stimulus appearance). The peak response should be higher than the mean + 5SD (SUA) or lower than the mean − 5SD (LFP) compared with the pre-stimulus activity (−100 ms time window before stimulus appearance). The visual RF was then determined by the area at half maximum around the center of RF. The size of the RF is represented by $r = \sqrt{RFarea/\pi}$, which is the radius of the RF assuming the circular RF. The eccentricity of the RF was defined as the distance between the fixational gaze position and the center of the RF. The same data were calculated again after they also transformed into SC coordinates based on the following formula to construct an RF map on the SC (Van Gisbergen *et al.*, 1987).

$$u = B_u \ln\left(\frac{\sqrt{R^2 + 2AR\cos(\phi)}}{A}\right)$$

$$v = B_v \arctan\left(\frac{R\sin(\phi)}{R\cos(\phi) + A}\right)$$

where u and v are the anatomical distances from the rostral pole (mm) along the horizontal axis and vertical axis, respectively. R is

the eccentricity in the visual space and φ is the meridianal direction of the target in the visual space. The constants are B_u = 1.4 mm, B_v = 1.8 mm/°, and A = 3°.

To further investigate the spatial properties of the visual response across time, we calculated the spatio-temporal response map using the same data set. We focused on the activity along a straight line between the fixational gaze position and the center of the RF. The activity for the location in space along this line was estimated by the same natural neighbor interpolation. For each data set, the location was normalised so that the fixational gaze position equaled 0 and the center of the RF equaled 1 (normalised eccentricity). The activity was also normalised so that the peak visual response equaled 1. These normalisations enabled us to compare the RF across different sessions. We then plotted the spatio-temporal RF using a 100 ms time window in 10 ms steps.

Results

Comparison between single unit activity and local field potential

We recorded SUA and the LFPs simultaneously from 111 sites in the SC of three monkeys. Of these, 53/111 (48%) were discarded from analysis, mostly because of significant artificial noise in the LFP; the remaining 58 sessions were analysed in detail. Figure 1C–F illustrates an example from the simultaneous recording of SUA and the LFP from one site in the SC. Both signals showed a significant phasic visual response that began shortly after stimulus appearance in the RF and a second peak of saccade-related activity around the initiation of saccades toward the RF. Note that the illustrated example had a saccade-related activity in the visual delay task (Fig. 1C and E) but not the memory delay task (Fig. 1D and F) as reported previously (Mohler & Wurtz, 1976; Mays & Sparks, 1980; Edelman & Goldberg, 2001). In addition, both signals had a significant post-saccadic visual response (Marino *et al.*, 2012) after saccade onset in the visual delay task only (Fig. 1C and E), and a significant visual off response at the time of stimulus disappearance in the memory delay task only (Fig. 1D and F). No significant responses were observed when the stimulus was presented in the anti-RF for both SUA and the LFP.

We classified visual neurons into two types based on the presence or absence of saccade-related activity (see Materials and methods): VIS neurons and VM neurons. Twenty neurons (34%) were classified as VIS because they had no significant saccadic activity in both the visual and memory delay tasks. Thirty-eight neurons (66%) were classified as VM because they had significant saccadic activity in the visual delay task. SUA and LFPs exhibited similar visual response properties, and these features were consistent across sessions. Figure 2 shows the population of the normalised SUA and LFP signals for each neuron type. The most notable thing was the similarity between SUA and LFP traces. Although the sessions were classified only by SUA, simultaneously recorded LFPs shared many of the same response properties as SUA. For example, LFPs recorded with VIS neurons had no observable saccade-related activity (Fig. 2A and B), whereas LFPs recorded with VM neurons had saccade-related activity in both visual delay and memory delay tasks (Fig. 2C and D).

We also compared the depth of each recording site (see Materials and methods). VIS neurons were recorded more superficially than VM neurons (Fig. 3A; VIS neuron, 0.45 ± 0.25 mm; VM neurons, 0.84 ± 0.36 mm; $P < 0.0001$, t-test). This suggested that VIS neurons were probably recorded from the SCs, whereas VM neurons were more likely to be in the SCi, which is consistent with many previous studies (Goldberg & Wurtz, 1972; Wurtz & Goldberg, 1972; Mohler & Wurtz, 1976; Mays & Sparks, 1980; Ma *et al.*, 1991; Munoz & Wurtz, 1995; McPeek & Keller, 2002). To test whether this layer difference was also found in the LFP, we calculated visuomotor indices for SUA and LFP in each session. The index shows the relative strength of visual and motor information in the signal. An index > 0 means that the signal contains visual information more than motor information, and an index < 0 means that the signal contains motor information more than visual information. As expected, SUA showed significant negative correlation between its visuomotor index and the depth of the recording site (Fig. 3B; $r = -0.677$, $P < 0.00001$). The LFP also showed weaker but significant correlation ($r = 0.269$, $P < 0.01$), indicating that the LFP also had layer differences, i.e. pure visual in the SCs and more saccadic in the SCi.

It is known that saccade-related activity of SC neurons is modulated by task; saccade-related activity is weaker or even absent from the same saccade neurons when the target is not visible at the time of saccade (Mohler & Wurtz, 1976; Mays & Sparks, 1980; Munoz & Wurtz, 1995; Edelman & Goldberg, 2001). Our results showed the same tendency in both SUA and LFP (Figs 1 and 2). To confirm this, we compared saccade-related activity (average normalised activity ±15 ms around saccade onset) between the visual delay and memory delay tasks (Fig. 3C). A 2 × 2 ANOVA (signals are, SUA and LFP; tasks are, visual delay and memory delay) showed a significant main effect of signal (SUA vs. LFP: $F_{1,228} = 0.8$, $P < 0.005$) and task (visual delay vs. memory delay: $F_{1,228} = 3.7$, $P < 1 \times 10^{-10}$), with a weak interaction effect ($F_{1,228} = 0.3$, $P < 0.05$). This suggested that both SUA and LFP had lower saccade-related activity in the memory delay task compared with the visual delay task. Figure 3D shows the task effect on saccade-related activity in each session. There was a significant correlation on task modulation between simultaneously recorded SUA and LFP pairs ($r = 0.42$, $P < 0.005$). Saccade-related activity tended to be weaker in the LFP compared with SUA; we found a higher visuomotor index in LFP ($P < 1 \times 10^{-5}$, sign test). However, the results showed that the sensory and motor properties of SUA were well preserved in the LFP, suggesting that the LFPs can be used as a representative neurophysiological signal in lieu of SUA in the SC.

Temporal and spatial properties of the visual response

Most of the neurons in the SC showed a strong phasic burst of action potentials that was time-locked to the appearance of visual stimuli in the RF. The RFs of neurons formed a retinotopic map in the SC (Cynader & Berman, 1972; Ottes *et al.*, 1986). We analysed the temporal and spatial properties of the visual response for SUA and LFPs. We compared the visual response onset latency, which was the time when the signal first differentiated from the baseline after stimulus appearance (see Materials and methods). The average visual response onset latency was 57.8 ± 14.0 ms for SUA and 56.5 ± 14.3 ms for the LFP (Fig. 4). We performed a 2 × 2 ANOVA for visual response onset latency (signals are, SUA and LFP; tasks are visual delay and memory delay), which showed no significant main effect of signal type (SUA vs. LFP: $F_{1,228} = 0.50$, $P > 0.4$) or task (visual delay vs. memory delay: $F_{1,228} = 0.04$, $P > 0.8$), indicating that SUA and LFP had similar temporal properties for visual response onset.

Next, to compare the spatial properties of the visual RF between SUA and LFP, we recorded SUA and LFP from 31 sites (16 of which were the same with previous recordings of visual delay and

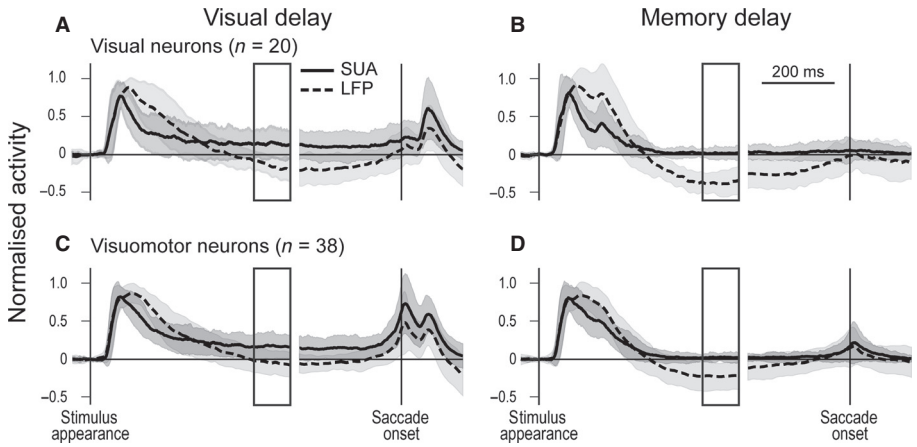

FIG. 2. Population histograms of SUA and LFP. Population histograms of the normalised activity of VIS neurons (n = 20) (A and B) and VM neurons (n = 38) (C and D). (A and C) Activity in the visual delay task. (B and D) Activity in the memory delay task. Solid lines indicate normalised SUA activity and dashed lines indicate normalised LFP activity. Signals were aligned to the stimulus appearance (left side) and saccade onset (right side). Shaded area represents the SD. Rectangles indicate the time windows for the delay epoch (solid) used in the following analysis.

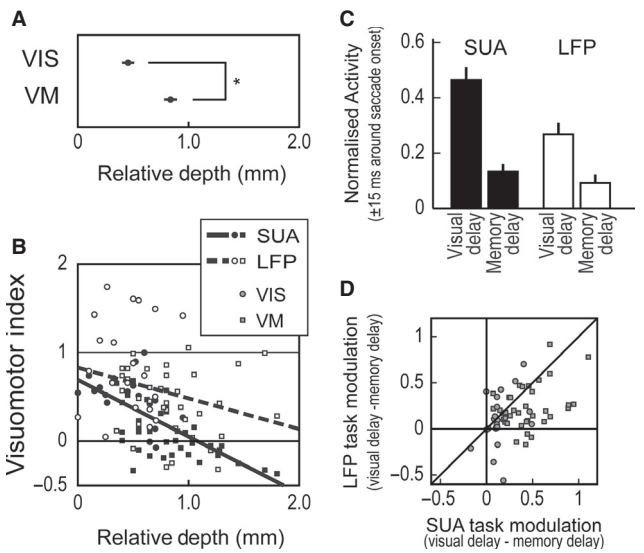

FIG. 3. Visuomotor properties of SUA and LFP. (A) The depth of the recording site from the surface of the SC for each type of neuron (mean ± SEM). *Statistically significant differences ($P < 0.001$, t-test). (B) Visuomotor index in each session for SUA (filled symbols) and LFP (open symbols). Lines show the result of simple linear regression (visuomotor index regressed by depth) for SUA (solid line) and LFP (dashed line). (C) Population comparison of saccade-related activity between SUA and LFP in visual and memory delay tasks. Error bars indicate SEM. (D) Session-based comparison of task modulation on saccade-related activity. Each symbol represents the data obtained from a single simultaneous recording. Circles indicate VIS neurons; squares indicate, VM neurons.

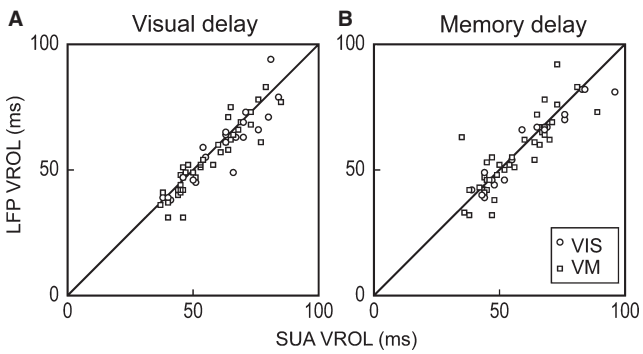

FIG. 4. Visual response onset latency (VROL) of SUA and LFP. Each symbol represents the data obtained from a single simultaneous recording in the visual delay task (A) and the memory delay task (B). Circles indicate VIS neurons; squares indicate VM neurons.

memory delay tasks) using a visual mapping task (see Materials and methods). Figure 5A–C shows an example of a single session (VM neuron). The locations of the visual stimulus positions relative to fixational gaze position are plotted in Fig. 5A and the time course of SUA and LFP activity at the center of the RF is plotted in Fig. 5B. Figure 5C shows the change of spatial properties of SUA (top panels) and LFP (bottom panels) across time. Both SUA and the LFP had a significant phasic visual response in a limited area (see RF in Fig. 5C, 50–150 ms). Population analysis showed that the SUA and LFP had largely overlapping visual RFs. Figure 6A compares the center of the RF for SUA and LFP. The distance between the RF centers for SUA and LFP was closely aligned and only differed by a few degrees (average 2.45 ± 2.01 deg), showing remarkable similarity between SUA and the LFP. LFPs tended to have larger RFs than SUA ($P < 0.01$, signed rank test). The size of the RF (see Materials and methods) was significantly correlated with the eccentricity of the RF (Fig. 6B; $r = 0.53$, $P < 0.01$ for SUA; $r = 0.39$, $P < 0.05$ for LFP), so we also compared the SUA and LFP RF size corrected by the eccentricity of the RF (RF size/RF eccentricity). Even when corrected for eccentricity, RF size remained significantly larger for LFP than SUA ($P < 0.01$, signed rank test; corrected RF size: 0.30 ± 0.05 for SUA and 0.41 ± 0.04 for LFP; mean ± SEM), indicating that RFs were, on average, 30–40% larger in diameter in the LFP compared with SUA.

We transformed the RFs from visual space into SC coordinates (Van Gisbergen *et al.*, 1987), and the estimated radius of the visual RF was larger for LFP than SUA (Fig. 6C; $P < 0.001$, signed rank test; 0.32 ± 0.03 mm for SUA and 0.46 ± 0.03 mm for LFP; mean ± SEM). The difference in size between SUA and LFP was 0.14 ± 0.16 mm, suggesting that the LFP represented the activity from a wider area in the SC (Katzner *et al.*, 2009), possibly reflecting the neurons at 100–200 μm around the recording site. However, there were no significant correlations between RF size in SC coordinate and the depth of the recording site for both SUA and the LFP (Fig. 6C; SUA, $r = 0.01$, $P > 0.9$; LFP, $r = -0.01$, $P > 0.9$). The

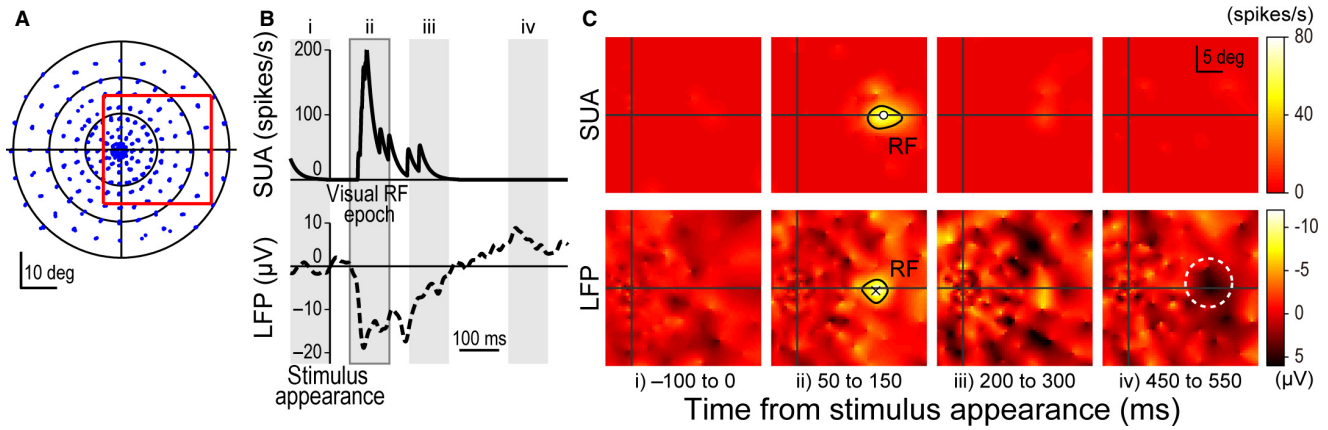

FIG. 5. Visual mapping task: example from a single session (VM neuron). (A) Stimulus locations in a session of 493 stimulus presentations. Each dot indicates stimulus locations relative to the gaze. Square indicates the mapped visual field highlighted in C. (B) Estimated SUA and LFP activity at the center of the visual RF by natural neighbor interpolation. Shaded areas indicate the four epochs used in C. (C) Spatial response map of SUA and LFP during four different epochs. White dot indicates center of SUA visual RF; cross mark indicates center of LFP visual RF; black circles indicate area of visual RF; white dotted circle indicates reversal of activity in the delay period.

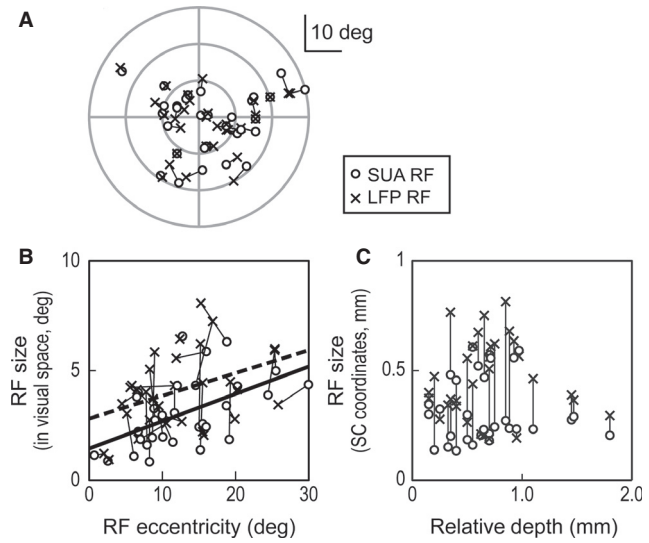

FIG. 6. Spatial properties of the visual RF in the SUA and LFP. (A) Comparison of center of visual RF between SUA and LFP. (B) Comparisons of size of visual RF between SUA and LFP. Open circles indicate SUA visual RF; cross marks indicate LFP visual RF. Lines show the result of simple linear regression (RF size regressed by RF eccentricity) for SUA (solid line) and LFP (dashed line). (C) Size of RF transformed into the SC coordinates plotted against depth of the recording site.

overall results indicated that SUA and LFP had similar spatial properties, although the RF tended to be larger for the LFP than SUA.

Suppressive after effect in the local field potential

We also examined differences between SUA and the LFP to see whether the LFP contained qualitatively different information from SUA. In Fig. 2, the LFP signals often dropped below baseline after the phasic visual response, whereas the SUA had a sustained response above baseline in the same period (delay period indicated by the empty rectangle boxes in Fig. 2). During the delay epoch (450–550 ms after stimulus appearance), the normalised SUA showed significant sustained activity (visual delay task: 0.16 ± 0.02, $P < 1 \times 10^{-5}$; memory delay task: 0.02 ± 0.01, $P < 0.05$; mean ± SEM, *t*-test corrected by Bonferroni method); however, the normalised LFP revealed significant suppression (visual delay task: -0.08 ± 0.02, $P < 0.01$; memory delay task: -0.27 ± 0.02, $P < 1 \times 10^{-5}$; mean ± SEM, *t*-test corrected by Bonferroni method). Figure 7 shows the details. A 2 × 2 ANOVA for the normalised SUA in the delay epoch (task: visual delay and memory delay; type: VIS and VM) showed a significant main effect of task (visual delay vs. memory delay: $F_{1,112} = 29.2$, $P < 1 \times 10^{-6}$) with no significant effect of type (VIS vs. VM: $F_{1,112} = 0.6$, $P > 0.4$) or interaction ($F_{1,112} = 0.3$, $P > 0.6$), suggesting that SUA had significantly higher sustained activity in the visual delay task, possibly reflecting the continuous visual input. However, a 2 × 2 ANOVA for the normalised LFP in the delay epoch (task: visual delay and memory delay; type: VIS and VM) showed a significant main effect of task (visual delay vs. memory delay: $F_{1,112} = 44.7$, $P < 1 \times 10^{-9}$) and type (VIS vs. VM: $F_{1,112} = 17.5$, $P < 0.0001$) with no significant interaction effect ($F_{1,112} = 0.6$, $P > 0.4$). This suggests that the suppressive effects were stronger in the memory delay task than the visual delay task, and more profound in the SCs than the SCi. To confirm this, we calculated the correlation coefficient between the delay epoch activity and the depth of the recording site (Fig. 7C and D). Although the LFP showed no significant correlation between the delay epoch activity and depth of the recording site in the visual delay task ($r = 0.15$, $P > 0.2$), there was a significant positive correlation in the memory delay task ($r = 0.36$, $P < 0.01$), supporting the idea that the suppressive effect of the LFP was stronger in the SCs compared with the SCi. SUA showed no significant correlation between the delay epoch activity and depth (visual delay task: $r = 0.03$, $P > 0.8$; memory delay task: $r = 0.2$, $P > 0.1$).

To visualise the changes of activation and suppression across time and space, we constructed a population spatio-temporal RF plot (Fig. 8) by normalising to the peak visual responses (see Materials and methods). The LFPs had larger visual RFs (vertical axis) confirming the previous observations (Fig. 6B). The LFPs showed a significant drop of activity only around the center of the RF at approximately 300 ms after stimulus appearance. This reversal of activity was significant at the center of the RF (average normalised response at 450–550 ms after stimulus appearance: -0.09 ± 0.24,

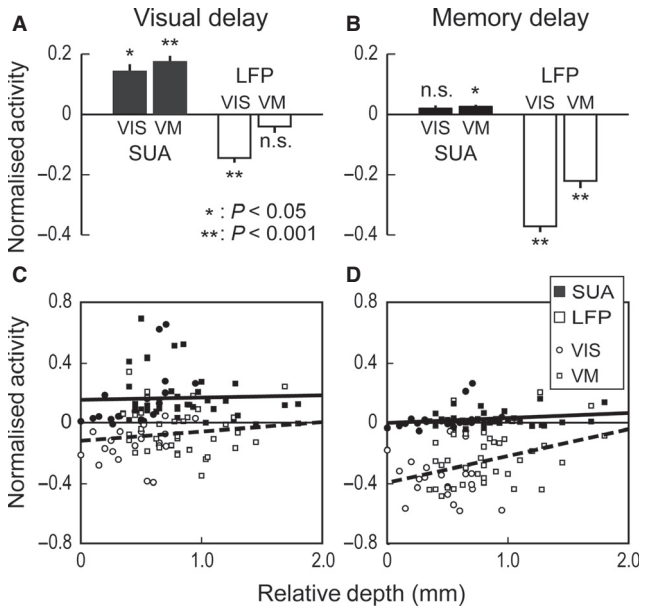

FIG. 7. Delay period activity of SUA and LFP. Population comparisons between SUA and LFP during delay epochs (450–550 ms after stimulus appearance) in visual delay task (A) and memory delay task (B). Black bars indicate normalised SUA and white bars indicate normalised LFP. For each bar, a one-sample *t*-test was conducted against zero (Bonferroni corrected). Error bars indicate SEM. (C and D) Delay epoch activity in each session plotted against depth of the recording site. Lines show the result of simple linear regression (normalised activity in the delay epoch regressed by depth) for SUA (solid line) and LFP (dashed line). Filled symbols indicate SUA; open symbols indicate LFP; circles indicate VIS neurons; squares indicate VM neurons. * and **Statistically significant differences ($P < 0.05$ and $P < 0.001$ by *t*-test, respectively).

$P < 0.05$, *t*-test). However, the drop of activity was strongest in the flanking points rather than the center of the RF. The average normalised activity at the ±15% eccentricity point from the center of the RF was significantly lower than at the center of the RF (-0.15 ± 0.22, $P < 0.05$, paired *t*-test at 85% amplitude point; -0.21 ± 0.23, $P < 0.05$, paired *t*-test at 115% amplitude point). The LFP showed surround suppression in the delay period, which is consistent with previous studies (Dorris *et al.*, 2007; Marino *et al.*, 2011; Phongphanphanee *et al.*, 2014).

Discussion

We recorded SUA and LFPs simultaneously from the primate SC and compared the temporal and spatial properties of the visual responses. If both signals were similar, then the LFP could be recommended as a reliable measure of neural activity in the SC, in lieu of SUA. Indeed, our results showed that SUA and accompanying LFPs had phasic visual responses with similar onset latencies and highly overlapping RFs. In addition, the LFP showed a significant reversal of activity after the phasic visual response, which indicated possible local suppression. We discuss the similarities and differences between SUA and LFP, and the possible neural mechanisms underlying these similarities and differences.

Visuomotor properties

The SC is a laminated structure with two functional regions. The SCs receive visual input from the retina and early visual cortex, whereas the intermediate layers (SCi) receive multisensory and cognitive input from various cortical areas, the basal ganglia, cerebellum, and SCs (White & Munoz, 2011). Neurons in the SCs are visual, whereas neurons in the SCi have multisensory responses (Stein & Meredith, 1993) and significant saccade-related activity (Mays & Sparks, 1980; Munoz & Wurtz, 1995). Similar to SUA, LFPs recorded in the SCs had a strong visual response without saccade-related activity, whereas LFPs recorded in the SCi had more saccade-related activity in addition to the visual response (Figs 2 and 3B). Thus, although LFPs reflect the neural activity within a few hundred micrometers around the recording site, they still capture important layer differences within the SC. LFPs also showed task-dependent modulation in a similar manner to SUA (Fig. 3D) (Mohler & Wurtz, 1976; Mays & Sparks, 1980; Munoz & Wurtz, 1995; Edelman & Goldberg, 2001), which is important in understanding the motor functions of the SC. The greatest difference was that saccade-related activity tended to be weaker in the LFP compared with SUA (Fig. 3C). Considering that SUA represents the output signal of the recorded neuron, whereas the LFP is more associated with the input (Mitzdorf, 1985; Buzsáki, 2004), this may suggest that saccade-related bursts are generated within the SC (Isa, 2002; Sparks, 2002), which determines the actual saccade parameters (Gandhi & Katnani, 2011). Several studies have shown how the SC is directly involved in the saccadic decision process, suggesting that saccade initiation occurs when the activity in the SCi reaches a certain threshold (Paré & Hanes, 2003; Bell *et al.*, 2005; Dorris *et al.*, 2007; Jantz *et al.*, 2013). Our results are consistent with this idea. The LFP for the saccade was typically weaker than the LFP for a visual response, suggesting a lack of synchrony of SCi input prior to a saccade. In other words, it may be the SCi itself that is accumulating the saccade trigger signal from integrating all of the diverse inputs.

Temporal properties of visual responses

It is widely accepted that LFPs mainly represent the local synaptic activity of all inputs to the recording site (Mitzdorf, 1985; Buzsáki, 2004; Logothetis & Wandell, 2004; Buzsáki *et al.*, 2012), whereas SUA reflects the output signal of the recorded neuron. Thus, one might assume that the LFP represents the first response to external events. Several previous studies have shown that the latency of the sensory response is shorter for LFP than SUA in the cerebral cortex (Noreña & Eggermont, 2002; Monosov *et al.*, 2008). However, we could not identify significant differences in latency between SUA and the LFP (Fig. 4). This might be because of the nature of the signals themselves; in the SC, the LFP is much noisier than SUA. The neurons in the SC have low spontaneous firing rates especially during visual fixation. Thus, baseline activity prior to stimulus onset was very low, which made it easy to detect the onset of the visual response with only a few spikes. However, the LFP had more variability even during the fixation period, thus it was more difficult to detect the precise onset of the visual response. This difference in signal-to-noise ratio may obscure any small onset latency difference between the LFP and SUA. However, it is reasonable to conclude that the phasic response of the LFP following visual stimulation coincided with the onset of SUA.

Spatial properties of the visual response

Simultaneously recorded SUA and LFP had very similar spatial patterns in the visual response. The RF centers were close in location, and the size of the RF scaled with the eccentricity of the RF for both signals (Fig. 5). The only significant difference was the size of the RF. The LFP tended to have a larger RF than SUA, which is

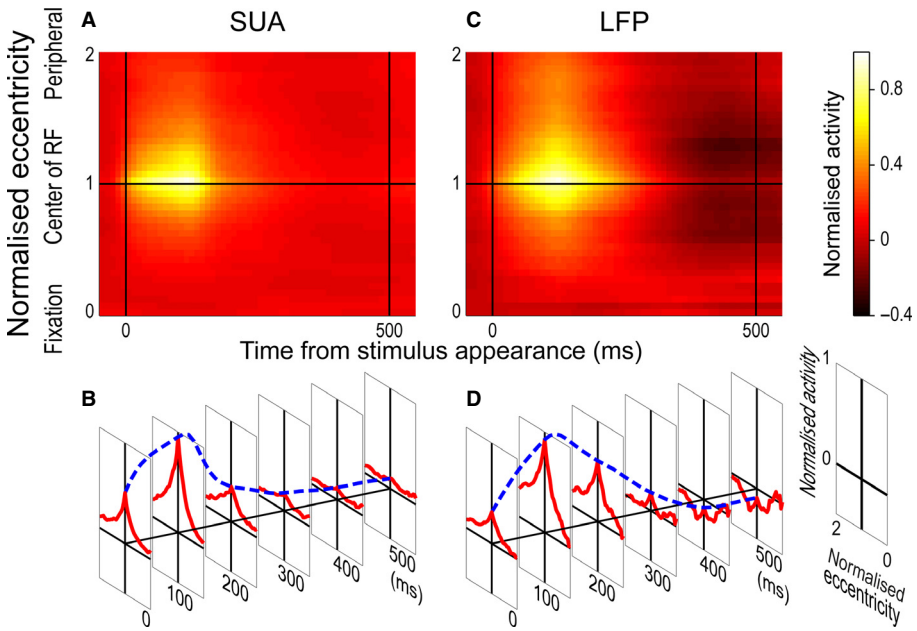

FIG. 8. Spatio-temporal activity plot of SUA and LFP. Average spatio-temporal response profiles of SUA (A) and LFP (C) for 31 sessions. (B and D) The three-dimensional plots of the spatio-temporal RF. Dashed lines indicate the average response at the center of RF across time. Solid lines indicate the average response at each time window across space.

reasonable considering that the LFP represents the population of activity of nearby neurons. This finding that RFs of the LFP are larger than those of SUA is similar to findings in the visual cortex (Katzner *et al.*, 2009; Xing *et al.*, 2009). However, the results indicate that the spatial information coded by SC neurons is well preserved within the LFP.

Suppressive effect in local field potential

We identified a difference between SUA and the LFP during the delay period, i.e. the LFP showed no sustained activity in the visual delay task, and exhibited a significant reversal of activity in the memory delay task that was absent in the SUA (Fig. 2). This reversal of activity indicates that the extracellular potential was higher than the baseline period, suggesting that the nearby neurons were hyperpolarised. Recently, a similar reversal of the LFP was found in the primary visual cortex of rodents (Haider *et al.*, 2013), which was actually accompanied by inhibition of nearby neurons. Thus, we suggest that the reversal of activity in the SC is also indicative of inhibition at the recording site. Considering that the suppression was restricted to a limited space around the center of the visual RF (Figs 5 and 8), we propose that the local inhibitory circuit within the SC is responsible for this suppressive effect observed in the LFPs. There are GABAergic interneurons within the SC (Mize *et al.*, 1991; Meredith & Ramoa, 1998; Lee *et al.*, 2001, 2007; Phongphanphanee *et al.*, 2011, 2014; Sooksawate *et al.*, 2011), and many of these project to the SCs and inhibit local excitatory neurons in the SCs (Lee *et al.*, 2007; Phongphanphanee *et al.*, 2011; Sooksawate *et al.*, 2011). Our results are consistent with these *in vitro* studies, thereby suggesting that the inhibitory effect observed in the LFP is mediated by the local inhibitory circuit within the SC. The SC also receives inhibitory inputs from the substantia nigra pars reticulata (Hikosaka & Wurtz, 1983a, 1985; Hikosaka *et al.*, 2000). However, the neurons in the substantia nigra have very broadly tuned RFs (Hikosaka & Wurtz, 1983b; Handel & Glimcher, 1999, 2000; Basso & Wurtz, 2002), and are thus less likely to be involved in the local suppressive effect. The visual mapping task revealed surround suppression during the delay period (Fig. 8), although there was no visual response during that period. This suggests that the surround suppression in the SC is functioning at the subthreshold level, which makes it difficult to assess by conventional SUA. The LFP might be able to provide access to local inhibitory effects within the SC.

We propose that the LFP in the SC represents the superposition of the excitatory inputs from various brain regions and local inhibitory inputs (Phongphanphanee *et al.*, 2014). The inhibitory inputs form surround suppression in both time and space, thereby improving resolution in the SC. Indeed, the visual response of SUA is suppressed by preceding visual stimuli presented at locations flanking the center of the RF (Churan *et al.*, 2012). The authors suggested a suppressive RF component by the visual stimulus, which had similar spatial properties to our results. Although their suppressive RF comes earlier (100–300 ms after stimulus onset), this difference in time is possibly due to the difference in visual stimulus used in the experiment as they used short flickering stimuli (85 Hz flickering) that were much shorter and possibly weaker than the stimuli that we used. The local suppression in the LFP that we found was relative to the pre-stimulus fixation period. SC neurons are tonically inhibited by nigrotectal and intra/intercollicular inhibition during the fixation (Hikosaka & Wurtz, 1983a; Peck, 1989; Dorris *et al.*, 1997; Meredith & Ramoa, 1998; Munoz & Istvan, 1998; Hikosaka *et al.*, 2000), which we could not see in the current analysis. We also did not identify significant suppression in the visual delay task, probably because of the continuous visual inputs during the delay period, which could have masked the suppression. What we found in the LFP is relative suppression induced by stimulus presentation that could be a part of the inhibitory interactions within the SC. Previous studies have suggested the importance of local inhibitory interactions in the SC for sensory [multisensory integration (Meredith & Stein, 1986, 1996), stimulus competition (Churan *et al.*, 2012),

sensory adaptation (Boehnke *et al.*, 2011; Dutta & Gutfreund, 2014)], motor [inhibition of return (Dorris *et al.*, 2002; Fecteau & Munoz, 2005; Ikeda *et al.*, 2011), saccade curvature (White *et al.*, 2011)], and cognitive [target selection (Li & Basso, 2005; Marino *et al.*, 2011)] function. Detailed analysis of LFPs may help in the understanding of the neural mechanisms underlying these various functions.

Acknowledgements

We acknowledge the outstanding technical assistance of Ann Lablans, Mike Lewis, and Sean Hickman, as well as members of the laboratory of D.P.M. for comments on an earlier version. This work was supported by an operating grant from the Canadian Institutes of Health Research (MOP-77734). D.P.M. was supported by the Canada Research Chair Program. The authors have no conflict of interests to declare.

Abbreviations

LFP, local field potential; RF, response field; SC, superior colliculus; SCi, intermediate layers of the superior colliculus; SCs, superficial layer of the superior colliculus; SUA, single unit activity; VIS, visual; VM, visuomotor.

References

Bahill, A.T., Kallman, J.S. & Lieberman, J.E. (1982) Frequency limitations of the two-point central difference differentiation algorithm. *Biol. Cybern.*, **45**, 1–4.

Basso, M.A. & Wurtz, R.H. (2002) Neuronal activity in substantia nigra pars reticulata during target selection. *J. Neurosci.*, **22**, 1883–1894.

Behan, M. & Appell, P.P. (1992) Intrinsic circuitry in the cat superior colliculus: projections from the superficial layers. *J. Comp. Neurol.*, **315**, 230–243.

Bell, A.H., Meredith, M.A., Van Opstal, A.J. & Munoz, D.P. (2005) Crossmodal integration in the primate superior colliculus underlying the preparation and initiation of saccadic eye movements. *J. Neurophysiol.*, **93**, 3659–3673.

Boehnke, S.E. & Munoz, D.P. (2008) On the importance of the transient visual response in the superior colliculus. *Curr. Opin. Neurobiol.*, **18**, 544–551.

Boehnke, S.E., Berg, D.J., Marino, R.A., Baldi, P.F., Itti, L. & Munoz, D.P. (2011) Visual adaptation and novelty responses in the superior colliculus. *Eur. J. Neurosci.*, **34**, 766–779.

Bullock, T.H. (1997) Signals and signs in the nervous system: the dynamic anatomy of electrical activity is probably information-rich. *Proc. Natl. Acad. Sci. USA*, **94**, 1–6.

Buzsáki, G. (2004) Large-scale recording of neuronal ensembles. *Nat. Neurosci.*, **7**, 446–451.

Buzsáki, G., Anastassiou, C.A. & Koch, C. (2012) The origin of extracellular fields and currents — EEG, ECoG, LFP and spikes. *Nat. Rev. Neurosci.*, **13**, 407–420.

Churan, J., Guitton, D. & Pack, C.C. (2012) Spatiotemporal structure of visual receptive fields in macaque superior colliculus. *J. Neurophysiol.*, **108**, 2653–2667.

Corneil, B.D. & Munoz, D.P. (2014) Overt responses during covert orienting. *Neuron*, **82**, 1230–1243.

Cynader, M. & Berman, N. (1972) Receptive-field organization of monkey superior colliculus. *J. Neurophysiol.*, **35**, 187–201.

Dorris, M.C., Pare, M. & Munoz, D.P. (1997) Neuronal activity in monkey superior colliculus related to the initiation of saccadic eye movements. *J. Neurosci.*, **17**, 8566–8579.

Dorris, M.C., Klein, R.M., Everling, S. & Munoz, D.P. (2002) Contribution of the primate superior colliculus to inhibition of return. *J. Cognitive Neurosci.*, **14**, 1256–1263.

Dorris, M.C., Olivier, E. & Munoz, D.P. (2007) Competitive integration of visual and preparatory signals in the superior colliculus during saccadic programming. *J. Neurosci.*, **27**, 5053–5062.

Dutta, A. & Gutfreund, Y. (2014) Saliency mapping in the optic tectum and its relationship to habituation. *Front. Integr. Neurosci.*, **8**, 1.

Edelman, J.A. & Goldberg, M.E. (2001) Dependence of saccade-related activity in the primate superior colliculus on visual target presence. *J. Neurophysiol.*, **86**, 676–691.

Einevoll, G.T., Kayser, C., Logothetis, N.K. & Panzeri, S. (2013) Modelling and analysis of local field potentials for studying the function of cortical circuits. *Nat. Rev. Neurosci.*, **14**, 770–785.

Fecteau, J.H. & Munoz, D.P. (2005) Correlates of capture of attention and inhibition of return across stages of visual processing. *J. Cognitive Neurosci.*, **17**, 1714–1727.

Fries, W. (1984) Cortical projections to the superior colliculus in the macaque monkey: a retrograde study using horseradish peroxidase. *J. Comp. Neurol.*, **230**, 55–76.

Gandhi, N.J. & Katnani, H.A. (2011) Motor functions of the superior colliculus. *Annu. Rev. Neurosci.*, **34**, 205–231.

Goldberg, M.E. & Wurtz, R.H. (1972) Activity of superior colliculus in behaving monkey. I. Visual receptive fields of single neurons. *J. Neurophysiol.*, **35**, 542–559.

Graybiel, A.M. (1978) Organization of the nigrotectal connection: an experimental tracer study in the cat. *Brain Res.*, **143**, 339–348.

Haider, B., Häusser, M. & Carandini, M. (2013) Inhibition dominates sensory responses in the awake cortex. *Nature*, **493**, 97–100.

Handel, A. & Glimcher, P.W. (1999) Quantitative analysis of substantia nigra pars reticulata activity during a visually guided saccade task. *J. Neurophysiol.*, **82**, 3458–3475.

Handel, A. & Glimcher, P.W. (2000) Contextual modulation of substantia nigra pars reticulata neurons. *J. Neurophysiol.*, **83**, 3042–3048.

Hikosaka, O. & Wurtz, R.H. (1983a) Visual and oculomotor functions of monkey substantia nigra pars reticulata. IV. Relation of substantia nigra to superior colliculus. *J. Neurophysiol.*, **49**, 1285–1301.

Hikosaka, O. & Wurtz, R.H. (1983b) Visual and oculomotor functions of monkey substantia nigra pars reticulata. I. Relation of visual and auditory responses to saccades. *J. Neurophysiol.*, **49**, 1230–1253.

Hikosaka, O. & Wurtz, R.H. (1985) Modification of saccadic eye movements by GABA-related substances. II. Effects of muscimol in monkey substantia nigra pars reticulata. *J. Neurophysiol.*, **53**, 292–308.

Hikosaka, O., Takikawa, Y. & Kawagoe, R. (2000) Role of the basal ganglia in the control of purposive saccadic eye movements. *Physiol. Rev.*, **80**, 953–978.

Ikeda, T., Yoshida, M. & Isa, T. (2011) Lesion of primary visual cortex in monkey impairs the inhibitory but not the facilitatory cueing effect on saccade. *J. Cognitive Neurosci.*, **23**, 1160–1169.

Isa, T. (2002) Intrinsic processing in the mammalian superior colliculus. *Curr. Opin. Neurobiol.*, **12**, 668–677.

Jantz, J.J., Watanabe, M., Everling, S. & Munoz, D.P. (2013) Threshold mechanism for saccade initiation in frontal eye field and superior colliculus. *J. Neurophysiol.*, **109**, 2767–2780.

Katzner, S., Nauhaus, I., Benucci, A., Bonin, V., Ringach, D.L. & Carandini, M. (2009) Local origin of field potentials in visual cortex. *Neuron*, **61**, 35–41.

Knudsen, E.I. (2011) Control from below: the role of a midbrain network in spatial attention. *Eur. J. Neurosci.*, **33**, 1961–1972.

Kuypers, H.G.J.M. & Lawrence, D.G. (1967) Cortical projections to the red nucleus and the brain stem in the rhesus monkey. *Brain Res.*, **4**, 151–188.

Lee, P.H., Helms, M.C., Augustine, G.J. & Hall, W.C. (1997) Role of intrinsic synaptic circuitry in collicular sensorimotor integration. *Proc. Natl. Acad. Sci. USA*, **94**, 13299–13304.

Lee, P.H., Schmidt, M. & Hall, W.C. (2001) Excitatory and inhibitory circuitry in the superficial gray layer of the superior colliculus. *J. Neurosci.*, **21**, 8145–8153.

Lee, P.H., Sooksawate, T., Yanagawa, Y., Isa, K., Isa, T. & Hall, W.C. (2007) Identity of a pathway for saccadic suppression. *Proc. Natl. Acad. Sci. USA*, **104**, 6824–6827.

Li, X. & Basso, M.A. (2005) Competitive stimulus interactions within single response fields of superior colliculus neurons. *J. Neurosci.*, **25**, 11357–11373.

Logothetis, N.K. & Wandell, B.A. (2004) Interpreting the BOLD Signal. *Annu. Rev. Physiol.*, **66**, 735–769.

Lui, F., Gregory, K.M., Blanks, R.H.I. & Giolli, R.A. (1995) Projections from visual areas of the cerebral cortex to pretectal nuclear complex, terminal accessory optic nuclei, and superior colliculus in macaque monkey. *J. Comp. Neurol.*, **363**, 439–460.

Ma, T.P., Graybiel, A.M. & Wurtz, R.H. (1991) Location of saccade-related neurons in the macaque superior colliculus. *Exp. Brain Res.*, **85**, 21–35.

Marino, R.A., Rodgers, C.K., Levy, R. & Munoz, D.P. (2008) Spatial relationships of visuomotor transformations in the superior colliculus map. *J. Neurophysiol.*, **100**, 2564–2576.
Marino, R.A., Trappenberg, T.P., Dorris, M. & Munoz, D.P. (2011) Spatial interactions in the superior colliculus predict saccade behavior in a neural field model. *J. Cognitive Neurosci.*, **24**, 315–336.
Marino, R.A., Levy, R., Boehnke, S., White, B.J., Itti, L. & Munoz, D.P. (2012) Linking visual response properties in the superior colliculus to saccade behavior. *Eur. J. Neurosci.*, **35**, 1738–1752.
Mays, L.E. & Sparks, D.L. (1980) Dissociation of visual and saccade-related responses in superior colliculus neurons. *J. Neurophysiol.*, **43**, 207–232.
McPeek, R.M. & Keller, E.L. (2002) Saccade target selection in the superior colliculus during a visual search task. *J. Neurophysiol.*, **88**, 2019–2034.
Meredith, M.A. & Ramoa, A.S. (1998) Intrinsic circuitry of the superior colliculus: pharmacophysiological identification of horizontally oriented inhibitory interneurons. *J. Neurophysiol.*, **79**, 1597–1602.
Meredith, M.A. & Stein, B.E. (1986) Visual, auditory, and somatosensory convergence on cells in superior colliculus results in multisensory integration. *J. Neurophysiol.*, **56**, 640–662.
Meredith, M.A. & Stein, B.E. (1996) Spatial determinants of multisensory integration in cat superior colliculus neurons. *J. Neurophysiol.*, **75**, 1843–1857.
Mitzdorf, U. (1985) Current source-density method and application in cat cerebral cortex: investigation of evoked potentials and EEG phenomena. *Physiol. Rev.*, **65**, 37–100.
Mize, R.R., Jeon, C.-J., Hamada, O.L. & Spencer, R.F. (1991) Organization of neurons labeled by antibodies to gamma-aminobutyric acid (GABA) in the superior colliculus of the Rhesus monkey. *Visual Neurosci.*, **6**, 75–92.
Mohler, C.W. & Wurtz, R.H. (1976) Organization of monkey superior colliculus: intermediate layer cells discharging before eye movements. *J. Neurophysiol.*, **39**, 722–744.
Monosov, I.E., Trageser, J.C. & Thompson, K.G. (2008) Measurements of simultaneously recorded spiking activity and local field potentials suggest that spatial selection emerges in the frontal eye field. *Neuron*, **57**, 614–625.
Moschovakis, A.K., Karabelas, A.B. & Highstein, S.M. (1988) Structure-function relationships in the primate superior colliculus. I. Morphological classification of efferent neurons. *J. Neurophysiol.*, **60**, 232–262.
Munoz, D.P. & Istvan, P.J. (1998) Lateral inhibitory interactions in the intermediate layers of the monkey superior colliculus. *J. Neurophysiol.*, **79**, 1193–1209.
Munoz, D.P. & Wurtz, R.H. (1995) Saccade-related activity in monkey superior colliculus. I. Characteristics of burst and buildup cells. *J. Neurophysiol.*, **73**, 2313–2333.
Noreña, A. & Eggermont, J.J. (2002) Comparison between local field potentials and unit cluster activity in primary auditory cortex and anterior auditory field in the cat. *Hearing Res.*, **166**, 202–213.
Oostenveld, R., Fries, P., Maris, E. & Schoffelen, J.-M. (2011) FieldTrip: open source software for advanced analysis of MEG, EEG, and invasive electrophysiological data. *Comput. Intell. Neurosci.*, **2011**, 156869.
Ottes, F.P., Van Gisbergen, J.A. & Eggermont, J.J. (1986) Visuomotor fields of the superior colliculus: a quantitative model. *Vision Res.*, **26**, 857–873.
Paré, M. & Hanes, D.P. (2003) Controlled movement processing: superior colliculus activity associated with countermanded saccades. *J. Neurosci.*, **23**, 6480–6489.
Peck, C.K. (1989) Visual responses of neurones in cat superior colliculus in relation to fixation of targets. *J. Physiol.*, **414**, 301–315.
Perry, V.H. & Cowey, A. (1984) Retinal ganglion cells that project to the superior colliculus and pretectum in the macaque monkey. *Neuroscience*, **12**, 1125–1137.
Phongphanphanee, P., Mizuno, F., Lee, P.H., Yanagawa, Y., Isa, T. & Hall, W.C. (2011) A circuit model for saccadic suppression in the superior colliculus. *J. Neurosci.*, **31**, 1949–1954.
Phongphanphanee, P., Marino, R.A., Kaneda, K., Yanagawa, Y., Munoz, D.P. & Isa, T. (2014) Distinct local circuit properties of the superficial and intermediate layers of the rodent superior colliculus. *Eur. J. Neurosci.*, **40**, 2329–2343.
Robinson, D.A. (1963) A method of measuring eye movement using a scleral search coil in a magnetic field. *IEEE T. Bio-med. Eng.*, **10**, 137–145.
Selemon, L. & Goldman-Rakic, P. (1988) Common cortical and subcortical targets of the dorsolateral prefrontal and posterior parietal cortices in the rhesus monkey: evidence for a distributed neural network subserving spatially guided behavior. *J. Neurosci.*, **8**, 4049–4068.
Sooksawate, T., Isa, K., Behan, M., Yanagawa, Y. & Isa, T. (2011) Organization of GABAergic inhibition in the motor output layer of the superior colliculus. *Eur. J. Neurosci.*, **33**, 421–432.
Sparks, D.L. (2002) The brainstem control of saccadic eye movements. *Nat. Rev. Neurosci.*, **3**, 952–964.
Stein, B.E. & Meredith, M. (1993) *The Merging of the Senses*, Cognitive neuroscience. The MIT Press, Cambridge.
Thompson, K.G., Hanes, D.P., Bichot, N.P. & Schall, J.D. (1996) Perceptual and motor processing stages identified in the activity of macaque frontal eye field neurons during visual search. *J. Neurophysiol.*, **76**, 4040–4055.
Van Gisbergen, J.A.M., Van Opstal, A.J. & Tax, A.A.M. (1987) Collicular ensemble coding of saccades based on vector summation. *Neuroscience*, **21**, 541–555.
Wässle, H. & Illing, R.-B. (1980) The retinal projection to the superior colliculus in the cat: a quantitative study with HRP. *J. Comp. Neurol.*, **190**, 333–356.
White, B.J. & Munoz, D.P. (2011) The superior colliculus. *The Oxford Handbook of Eye Movements*. 1st Edn. pp. 195–213. Oxford University Press, Oxford, UK.
White, B.J., Theeuwes, J. & Munoz, D.P. (2011) Interaction between visual- and goal-related neuronal signals on the trajectories of saccadic eye movements. *J. Cognitive Neurosci.*, **24**, 707–717.
Wurtz, R.H. & Goldberg, M.E. (1972) Activity of superior colliculus in behaving monkey. III. Cells discharging before eye movements. *J. Neurophysiol.*, **35**, 575–586.
Xing, D., Yeh, C.-I. & Shapley, R.M. (2009) Spatial spread of the local field potential and its laminar variation in visual cortex. *J. Neurosci.*, **29**, 11540–11549.
Zanos, T.P., Mineault, P.J. & Pack, C.C. (2011) Removal of spurious correlations between spikes and local field potentials. *J. Neurophysiol.*, **105**, 474–486.